

# Recovery of spectral features readout with frequency-chirped laser fields

Tiejun Chang, Mingzhen Tian, R. Krishna Mohan, Christoffer Renner,  
Kristian D. Merkel, and W. Randall Babbitt

*Spectrum Laboratory and Department of Physics, Montana State University, Bozeman, Montana 59717*

Received October 19, 2004

A data-processing technique is proposed for use with conventional frequency-chirped absorption spectroscopy to ensure accurate mapping of spectral features into time-domain signatures with arbitrarily fast readout chirp rates. This technique recovers the spectrum from a signal that is distorted owing to the fast chirp rate and therefore facilitates fast measurement of the spectral features over a broad spectral range with high resolution. Both numerical simulations and experimental results are presented. © 2005 Optical Society of America

OCIS codes: 300.1030, 070.0070, 020.1670.

Conventional absorption spectroscopy and coherent transient spectroscopy<sup>1-9</sup> are commonly used techniques for the readout of spectral features. In coherent transient spectroscopy, a Fourier-transform-limited laser field, usually a brief pulse, is used to probe the medium. The output field contains a high-bandwidth coherent response from the spectral features.<sup>3</sup> This technique has limited practical utility, as it requires high-power and high-bandwidth laser sources and low-noise and high-dynamic-range broad-bandwidth photodetectors. In conventional absorption spectroscopy, a frequency-chirped electric field is used to attempt to create a temporal map of the spectral features. However, the readout chirp rate is limited if high spectral resolution is required. Mapping a Lorentzian spectral hole with FWHM  $\Gamma$  requires that  $\kappa \ll \Gamma^2$ , where  $\kappa = B/\tau_c$  is the chirp rate for chirp bandwidth  $B$  and chirp time  $\tau_c$ . When the chirp rate is fast relative to the spectral features of interest, the readout signal deviates from direct mapping owing to the coherent response from the medium. We propose a data-processing technique to remove these distortions such that the spectral features can be recovered with fast readout and high resolution.

The propagation of electric field  $E$  along direction  $z$  through a material is described by  $\partial^2 E/\partial z^2 - \mu_0 \epsilon_0 \partial^2 E/\partial t^2 = \mu_0 \partial^2 P/\partial t^2$ , where  $P$  is the polarization and  $\epsilon_0$  and  $\mu_0$  are the electric permittivity and magnetic permeability, respectively, of free space. Applying the slowly varying envelope approximation in a rotating frame with  $E = E(t, z) \cos(2\pi\nu_0 t - k_0 z)$  and  $P = P(t, z) \cos(2\pi\nu_0 t - k_0 z)$  and transforming to a moving coordinate system ( $z \rightarrow z, t \rightarrow t - z/c$ ) yields  $\partial E(t, z)/\partial z = -i\mu_0 \pi \nu_0 c P(t, z)$ , where  $\nu_0$  is the optical carrier frequency,  $k_0 = 2\pi\nu_0/c$ , and  $c = 1/\sqrt{\epsilon_0 \mu_0}$ . For an optically thin medium of length  $dz$ , the field propagation can be simplified as  $E^{\text{out}}(t) = E^{\text{in}}(t) - idz\mu_0 \pi \nu_0 c P(t)$ . The polarization is now  $z$  independent and is related to the incident field by  $P(v) = \epsilon_0 \chi(v) E(v)$ , where  $E(v)$  and  $P(v)$  are the Fourier transforms of  $E(t)$  and  $P(t)$ , respectively, and  $\chi(v) = \chi'(v) + i\chi''(v)$  is the complex susceptibility of the ma-

terial, which is related to absorption coefficient  $\alpha(v)$  as  $\chi''(v) \approx -\alpha(v)/k_0$  and  $\chi'(v) = (2/\pi) \int_{-\infty}^{\infty} s \chi''(s)/(s^2 - v^2) ds$ . In general, any arbitrary spectral features can be decomposed as  $\alpha(v) = \int_0^{\infty} \gamma(\tau) \cos[2\pi\nu\tau + \varphi(\tau)] d\tau$ . Within the context of spectral holography,  $\alpha(v)$  can be viewed as a series of sinusoidal spectral gratings with a corresponding period of  $1/\tau$ , where  $\gamma(\tau)$  is the spectral grating amplitude and  $\varphi(\tau)$  is the phase of the spectral grating. The complex susceptibility and the polarization can now be expressed as  $\chi(v) = (i/k_0) \int_0^{\infty} \gamma(\tau) \exp\{-i[2\pi\nu\tau + \varphi(\tau)]\} d\tau$  and  $P(t) = \epsilon_0 \int_0^{\infty} \chi(\tau) E(t - \tau) d\tau$ , where  $\chi(\tau) = (i/k_0) \gamma(\tau) \exp[-i\varphi(\tau)]$ . The resultant output field from the material is

$$E^{\text{out}}(t) = E^{\text{in}}(t) - dz \int_0^{\infty} \gamma(\tau) \exp[-i\varphi(\tau)] E^{\text{in}}(t - \tau) d\tau. \quad (1)$$

For chirped readout the input probe field is  $E_c^{\text{in}}(t) = E_0 \cos(2\pi\nu_s t + \kappa t^2/2)$ , where  $E_0$  is the amplitude of the field and  $\nu_s$  is the start frequency of the chirp. The output is the sum of the delayed weighted replicas of the chirped pulses and the transmitted chirped pulse. The intensity of the readout signal is

$$|E_c^{\text{out}}(t)|^2 = E_0^2 + A \int_0^{\infty} \gamma(\tau) \cos[2\pi\kappa\tau + \phi_l + \phi_q + \varphi(\tau)] d\tau, \quad (2)$$

where  $A = -2E_0^2$ ,  $\phi_l = 2\pi\nu_s \tau$  is the start-frequency-dependent phase, and  $\phi_q = -\pi\kappa\tau^2$  is the quadratic phase. When  $\phi_q \ll \pi$  ( $\kappa\tau^2 \ll 1$ ), the second term of  $|E_c^{\text{out}}(t)|^2$  is proportional to  $\alpha(v)$ , with the frequency time-scale conversion  $v = \kappa t$  and an offset of  $\nu_s/\kappa$  that is due to  $\phi_l$ . The output is a direct map of the spectral features in the materials, as in conventional absorption spectroscopy. The quadratic phase,  $\phi_q$ , is responsible for the significant deviation from the direct spectral mapping for chirp rates of the order of  $1/\tau_{\text{max}}^2$  or greater,<sup>4</sup> where  $\tau_{\text{max}}$  is defined as  $\gamma(\tau) \approx 0$  for  $\tau > \tau_{\text{max}}$  and is related to the finest spectral features.

In the case of a single Lorentzian spectral hole with FWHM  $\Gamma$ ,  $\gamma(\tau) \propto \exp(-\Gamma\tau)$ , the distortion that is due to  $\phi_g$  can be ignored only when  $\kappa \ll \Gamma^2$ . In general, the slow chirp readout limit is relative to the finest structure of the spectral features.

A novel solution for the distorted chirp readout is to remove the quadratic phases from the readout signal in postprocessing. The procedure is as follows: (1) Fourier transform readout signal intensity  $|E_c^{\text{out}}(t)|^2$ , (2) compensate for the linear and quadratic phases, and (3) inverse Fourier transform the result of step (2). Step (1) yields

$$S(v) = [A\gamma(|v/\kappa|)/2\kappa] \exp\{i[2\pi v_s v/\kappa - \text{sgn}(v)\pi v^2/\kappa + \text{sgn}(v)\varphi(|v/\kappa|)]\}, \quad (3)$$

where  $\text{sgn}(v) = +1$  for  $v \geq 0$  and  $\text{sgn}(v) = -1$  for  $v < 0$ . In step (2) we compensate for the linear and the quadratic phases by multiplying  $S(v)$  by  $\exp\{-i\pi[2v_s v - \text{sgn}(v)v^2]/\kappa\}$ , which yields

$$S'(v) = A[\gamma(|v/\kappa|)/2\kappa] \exp[i \text{sgn}(v)\varphi(|v/\kappa|)]. \quad (4)$$

Phase  $\varphi(|v/\kappa|)$  and the grating amplitude  $\gamma(|v/\kappa|)$  are functions of the delay,  $\tau_v = |v/\kappa|$ , and carry complete information on the original spectral features. Step (3) yields the restored spectrum:

$$S(t) = A \int_0^\infty \gamma(\tau_v) \cos[2\pi\tau_v\kappa t + \varphi(\tau_v)] d\tau_v = A\alpha(\kappa t), \quad (5)$$

which is an exact mapping of  $\alpha(v - v_s)$ . This algorithm enables arbitrary spectral features to be recovered with arbitrarily fast readout chirp rates, provided that the chirp bandwidth covers the full spectrum of interest and that there is an additional bandwidth of  $\approx \kappa/\delta v$ , where  $\delta v$  is the finest feature width. Therefore the spectral resolution of the recovery algorithm,  $\delta v = \tau_c^{-1}$ , is determined by the chirp duration instead of by the chirp rate.

Using a previously developed numerical model for inhomogeneously broadened media,<sup>8</sup> we simulated the readout and recovery of Lorentzian spectral holes of various widths with a readout chirp rate of  $\kappa = 1 \text{ MHz}/\mu\text{s}$ . The normalized readout signals and the normalized spectral holes are plotted in the upper parts of curves (a)–(d) in Fig. 1 for  $\Gamma = 3, 1, 0.3, 0.1 \text{ MHz}$ . The temporal profiles of the readout signals are plotted on the converted frequency scale. The recovered spectra are the lower parts of the curves in the figure. In curves (d) and (c),  $\kappa \gg \Gamma^2$  and the readout signals are severely distorted. Even when  $\kappa = \Gamma^2$  as in curve (b), the distortions are still significant. Only when  $\kappa \ll \Gamma^2$ , as in curve (a), is the direct mapping condition of conventional absorption spectroscopy close to being met, though a slight distortion is still noticeable. In all cases the recovery algorithm produced accurate mappings of the spectral feature.

This spectral recovery technique was experimentally demonstrated with a spectral hole-burning crystal,  $\text{Tm}^{3+}:\text{YAG}$ , at 4.2 K. Figure 2(a) shows a sche-

matic of the experimental setup. A frequency-stabilized diode laser is tuned to the absorption resonance of  $\text{Tm}^{3+}$  at 793.380 nm. A radio-frequency (RF) signal from the arbitrary wave-form generator (AWG) was modulated onto the optical carrier by an acousto-optic modulator (AOM). The crystal was irradiated with the modulated light for 100  $\mu\text{s}$ . Spectral holes that are due to driving the AOM with frequencies of 262, 263, 264, and 270 MHz are engraved in the crystal. The hole widths, estimated at 200 kHz, result from the recording time, the laser linewidth, and the coherence decay time ( $\sim 20 \mu\text{s}$ ). Two digital chirps of bandwidth  $B = 20 \text{ MHz}$  were generated with the AOM driven by the AWG. The chirp durations,  $\tau_c$ , were 100  $\mu\text{s}$  ( $\kappa = 0.2 \text{ MHz}/\mu\text{s}$ ) and 20  $\mu\text{s}$  ( $\kappa = 1 \text{ MHz}/\mu\text{s}$ ). These chirp rates are 5 times and 25 times faster, respectively, than the conventional limit given by  $\Gamma^2 \approx 0.04 \text{ MHz}/\mu\text{s}$ . The readout signals, on a

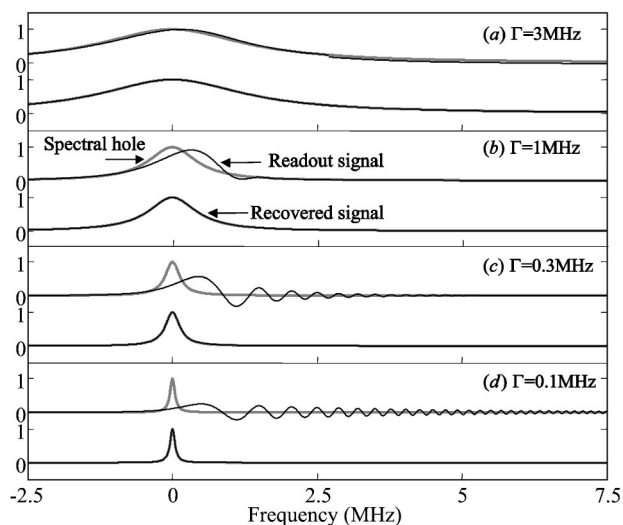


Fig. 1. Simulations of chirped readout ( $\kappa = 1 \text{ MHz}/\mu\text{s}$ ) of spectral holes of various widths. The normalized readout and recovered signals are plotted as a function of frequency for comparison with the normalized spectral hole. The recovery processing uses the readout data with a bandwidth from  $-10$  to  $10 \text{ MHz}$ . To show the details of the signal, the frequency scale in the plot is from  $-2.5$  to  $7.5 \text{ MHz}$ .

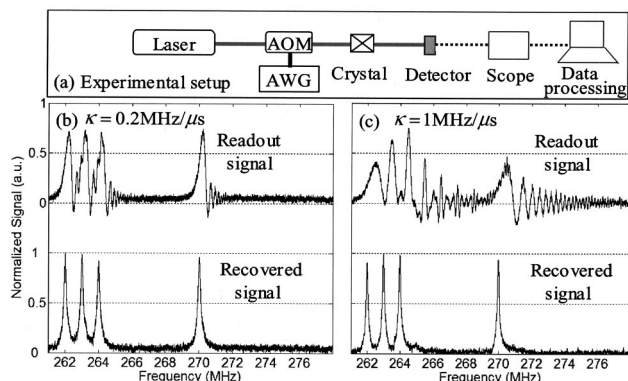


Fig. 2. Experimental demonstration: (a) schematic of the experimental setup. Readout and recovered signals with (b)  $\kappa = 0.2$  and (c)  $\kappa = 1 \text{ MHz}/\mu\text{s}$ .

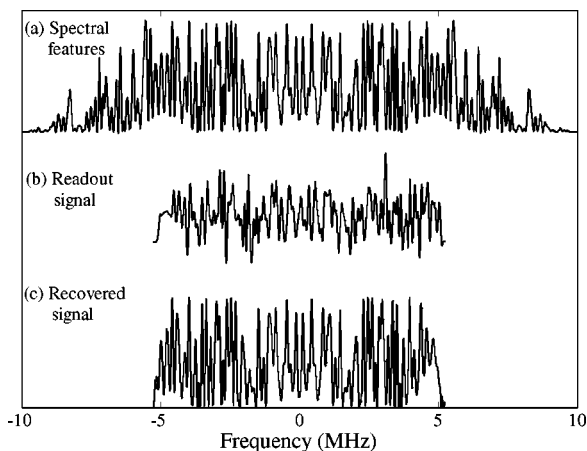


Fig. 3. Simulation of chirped readout of an arbitrary spectrum. (a) An arbitrary spectrum with finest feature  $\delta\nu \approx 0.1$  MHz. (b) A readout signal with  $B=10$  MHz and  $\kappa=1$  MHz/ $\mu$ s. (c) The recovered spectrum.

converted frequency scale, are shown in the upper traces of Figs. 2(b) and 2(c). In the readout signal with  $\kappa=0.2$  MHz/ $\mu$ s, the frequencies of primary spectral features can be resolved but the shapes are distorted. The readout signal with  $\kappa=1$  MHz/ $\mu$ s has significant distortions that are due to the interference between the coherent responses, and the frequencies of the spectral features cannot be resolved. The lower traces in Figs. 2(b) and 2(c) show the recovered signals that are almost identical for these two chirp rates. The small differences are due to fluctuations during burning and readout.

To demonstrate the readout of arbitrary absorption spectral features we simulated the readout of a complicated spectral profile in Fig. 3(a), which we created by using a pseudorandom biphasic pattern at 10 Mbits/s with a pattern duration of  $\tau_p=10$   $\mu$ s. As the material's coherence decay is ignored, the finest feature,  $\delta\nu \approx 0.1$  MHz, is determined by the pattern duration. The readout chirp has bandwidth  $B=10.4$  MHz and chirp duration  $\tau_c=104$   $\mu$ s, which includes rising and falling edges of 2  $\mu$ s each and corresponding frequency scanning of 0.2 MHz each. The chirp rate,  $\kappa=0.1$  MHz/ $\mu$ s, is ten times faster than the slow chirp limit  $\delta\nu^2$ ; this causes significant deviation of the direct readout signal in curve (b) of Fig. 3 from the original spectrum in curve (a). The recovered data, plotted in curve (c) of Fig. 3, is a precise map of the spectral features over the center bandwidth. One can correct the distortions on the rising edge that result from the nonuniform amplitude by normalizing the recovered signal with the chirp field envelope. However, distortions near the falling edge result not only from the nonuniform amplitude but also from a cutoff effect. The information about each spectral feature is spread out in the readout signal over a temporal duration up to  $\tau_p \approx 1/\delta\nu$ . The cutoff in time affects the accuracy of the mapping in the frequency range up to  $\kappa\tau_p$  from the falling edge, which is 1 MHz in this case.

The recovery algorithm permits fast measurement of spectral features over a broad spectral range with high resolution and eliminates the need for prior knowledge of the spectral feature to adjust the chirp rate, as required by conventional absorption spectroscopy. Spectral features over a bandwidth  $B$  can be measured with chirp rates up to  $\kappa=B\delta\nu$ , where  $\delta\nu$  is the finest possible feature width that can be estimated from the recording time, laser linewidth, and homogeneous broadening. This chirp rate is  $B/\delta\nu$  times faster than  $\delta\nu^2$ , the limit of conventional absorption spectroscopy. The requirement of the detector bandwidth increases with the readout chirp rate. To resolve minimum spectral feature  $\delta\nu$  by using a chirp with rate  $\kappa$ , we require the detector to have a bandwidth  $\kappa\delta\nu^{-1}$ . For maximum chirp rate  $\kappa=B\delta\nu$ , the detector bandwidth should be  $B$ , which is the same as that of coherent transient spectroscopy. Because the chirp readout uses heterodyne detection for which the output signal is the beat of the echo field and the transmitted field, the output signal is stronger than the direct detection of the echo signal used in coherent transient spectroscopy. Inasmuch as the recovery algorithm treats conventional absorption spectroscopy and coherent transient spectroscopy in the same physical framework, it is applicable for a vast range of chirp rates and provides flexibility in a variety of applications, including RF signal processing and RF spectral analysis.

We are grateful to Kelvin Wagner of the University of Colorado and Zachary Cole and Randy Reibel of the Spectrum Laboratory for helpful discussions. This research was supported by the Defense Advanced Research Projects Agency (grant MDA972-03-1-0002), U.S. Air Force Office of Scientific Research—Defense Experimental Program to Stimulate Competitive Research grant F49620-02-1-0275, and the Montana Board of Research and Commercialization Technology (grant 04-52). T. Chang's e-mail address is chang@spectrum.montana.edu.

## References

1. K. D. Merkel, R. K. Mohan, T. Chang, Z. Cole, A. Olson, and W. R. Babbitt, *J. Lumin.* **107**, 62 (2004).
2. C. M. Jefferson and A. J. Meixner, *Chem. Phys. Lett.* **189**, 60 (1992).
3. S. Mukamel, *Principles of Nonlinear Optical Spectroscopy* (Oxford U. Press, Oxford, 1995).
4. H. Lin, T. Wang, G. A. Wilson, and T. W. Mossberg, *Opt. Lett.* **15**, 928 (1995).
5. T. Chang, R. K. Mohan, M. Tian, T. L. Harris, Wm. R. Babbitt, and K. D. Merkel, *Phys. Rev. A* **70**, 063803 (2004).
6. F. Perdu, I. Lorgere, and J.-L. Le Guet, *Opt. Lett.* **25**, 669 (2000).
7. L. Menager, I. Lorgere, J.-L. Le Guet, D. Dolfi, and J.-P. Huignard, *Opt. Lett.* **26**, 1245 (2001).
8. T. Chang, M. Tian, Z. W. Barber, and W. R. Babbitt, *J. Lumin.* **107**, 138 (2004).
9. F. Schlottau and K. H. Wagner, *J. Lumin.* **107**, 90 (2004).